Available online at www.sciencedirect.com
ScienceDirect
Trans. Nonferrous Met. Soc. China 19(2009) 143−148
Transactions of Nonferrous Metals Society of China
www.tnmsc.cn

Microstructure and corrosion resistance of Fe-Al intermetallic coating on 45 steel synthesized by double glow plasma surface alloying technology

ZHU Xiao-lin(朱晓林), YAO Zheng-jun(姚正军), GU Xue-dong(顾雪冬),
CONG Wei(丛 伟), ZHANG Ping-ze(张平则)

College of Material Science and Technology, Nanjing University of Aeronautics and Astronautics, Nanjing 210016, China

Received 15 February 2008; accepted 2 July 2008

Abstract: A binary Fe-Al alloyed layer was synthesized on 45 steel by means of double glow plasma surface alloying technique. The corrosion-resisting layer prepared is composed of a sedimentary layer and a diffusion layer, with a total thickness of about 180 μm. The aluminum content of the alloyed layer shows gradual change from surface to the inside of substrate. The ideal profile is beneficial to the metallurgical bonding of the surface alloying layer with substrate materials. The microstructure of both layers consists of the Fe-Al intermetallic compound, which is FeAl with *B*2 structure in the sedimentary layer and Fe_3Al with incompletely ordered DO_3 structure in the diffusion layer. The protective film exhibits high micro-hardness. In comparison with the substrate of 45 steel, the corrosion resistance of the aluminized sample is much higher in 2.0% Na_2S and 0.05 mol/L Na_2SO_4 + 0.5 mol/L NaCl mixed solutions.

Key words: plasma surface alloying; Fe-Al intermetallic; 45 steel; corrosion resistance

1 Introduction

Fe-Al intermetallic compounds are regarded as promising materials for industrial applications because of their low cost, low density, high specific strength, high-temperature strength, as well as excellent oxidation and corrosion resistance[1−3]. However, it is difficult to fabricate components using massive Fe-Al based materials due to their poor castability and workability. Recently, surface coating technologies have been used to produce Fe-Al intermetallic anti-corrosion coatings on the surface of components, such as plasma spraying, laser cladding, and hot-dip aluminizing.

So far, the corrosion resistance of Fe-Al based alloys has been studied and reported systematically in literature. However, the previous investigations were mainly concentrated on oxidation and sulfidation at high temperatures, hot corrosion in molten salt and aqueous corrosion of Fe-Al-Cr(Mn, Ti, RE)-based complex alloys[4−8]. While only a little information has been obtained concerning the aqueous corrosion behavior of binary Fe-Al surface coating.

In the present work, the aluminizing process on 45 steel is conducted using double glow plasma surface alloying technology, and a Fe-Al intermetallic protective film is successfully formed on the surface of 45 steel. The microstructure, micro-hardness and aqueous corrosion behavior of the aluminized layer are studied.

2 Experimental

The material of the substrate for surface coating is commonly used 45 steel with the size of *d* 50 mm×7 mm. After mechanical polishing, the steel substrate was degreased using acetone. Pure aluminum (99.9%) was melted in a graphite crucible (*d* 80 mm×40 mm) used as the source electrode.

The Fe-Al intermetallic layer was prepared using self-made furnace, in which the temperature was monitored using a WGG2−201 type optical pyrometer. The processing parameters are listed in Table 1.

To observe the microstructure of the alloyed layer, the cross sections of samples with Fe-Al surface layer prepared were mechanically polished and then etched using a solution of 4 mL HNO_3 + 96 mL C_2H_5OH at

Foundation item: Project(BK2005128) supported by the Natural Science Foundation of Jiangsu Province, China
Corresponding author: YAO Zheng-Jun, Tel: +86-13951818597, E-mail: yaozj@nuaa.edu.cn
DOI: 10.1016/S1003-6326(08)60242-3

Table 1 Processing parameters

Source voltage/V	Workpiece voltage/V	Ar pressure/Pa	Distance between workpiece and source/mm	Temperature/℃	Holding time/h
950	400	35	20	950	3

room temperature. The microstructure observation of the surface layer prepared was performed using optical microscopy (OM) and scanning electron microscopy (SEM). Phase identification and microanalysis were conducted on the surface layer prepared using X-ray diffractometry (XRD) and energy dispersive spectroscopy (EDS), respectively. Shimadzu Dynamic Ultra-micro Hardness System (DUH−W201/W201S, Japan) configured with a Berkovich (3-sided pyramid, 100°) diamond tip nano-indenter was used to measure the dynamic hardness and elastic modulus of the substrate and aluminized layer.

The corrosion behavior of the aluminized layer was evaluated at 25 ℃, in comparison with substrate and 1Cr18Ni9Ti stainless steel, using CHI 660B type electrochemical workstation at a scanning rate of 0.002 V/s. The tests were conducted in 2.0%Na_2S solution and 0.05 mol/L Na_2SO_4 + 0.5 mol/L NaCl mixed solution in atmosphere. Three-electrode system was applied to determine the polarization curves. The alloyed layer was exposed in the solution as working electrode, with Pt as the auxiliary electrode and the saturated calomel electrode (SCE) as the reference electrode. The calculation of corrosion rate was on the basis of Faraday Law:

$$v=mJ_{corr}/nF$$

where v is the corrosion rate ($g\cdot m^{-2}\cdot h^{-1}$); m is the atomic mass (g); n is the valence of metal ion; F is Faraday constant (26.8 A·h) and J_{corr} is corrosion current density (A/m^2).

3 Results and discussion

3.1 Microstructure

Fig.1(a) shows the SEM image of the cross-section of the aluminized sample, from which it can be seen that the aluminized coating consists of two layers: a sedimentary layer and a diffusion layer marked as Ⅰ and Ⅱ, respectively. The sedimentary layer is loose and porous, while the diffusion layer is uniform and dense without cracks and holes. Fig.1(b) shows the enlarged image of interface between the substrate and the diffusion layer, from which a transition region between the diffusion layer and substrate can be clearly seen.

3.2 Chemical composition and phase identification

Fig.2 shows the result of EDS linear scanning performed on the cross section of the surface layer prepared. It can be seen that the Al content decreases

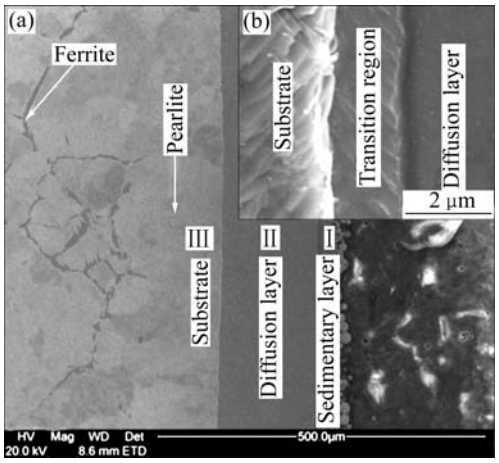

Fig.1 Cross-section microstructure of aluminized layer

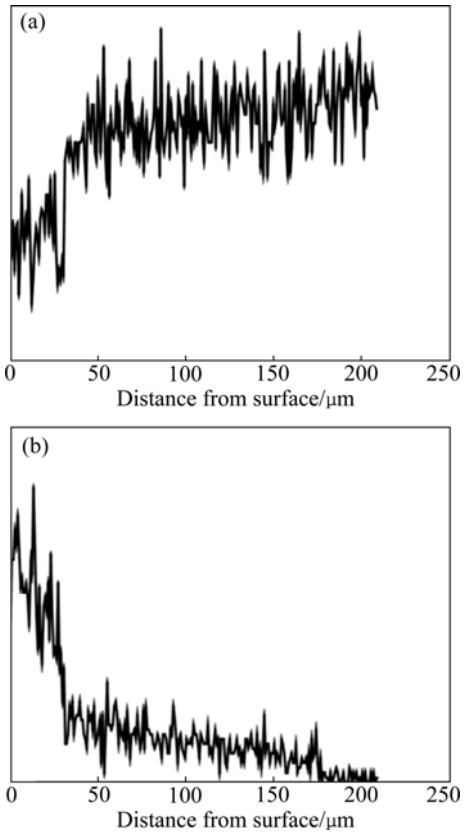

Fig.2 Content distribution of Fe (a) and Al (b) on cross section of surface layer

sharply in the region of 30 μm in width underneath the surface. According to Fig.1(a), this region should be the sedimentary layer. Fig.3(a) shows XRD pattern taken from the sample surface, in which all the peaks are indexed as arising from the Fe-Al intermetallic compound. According to the Fe-Al binary diagram, there are two types of Fe-Al intermetallic phases, FeAl and

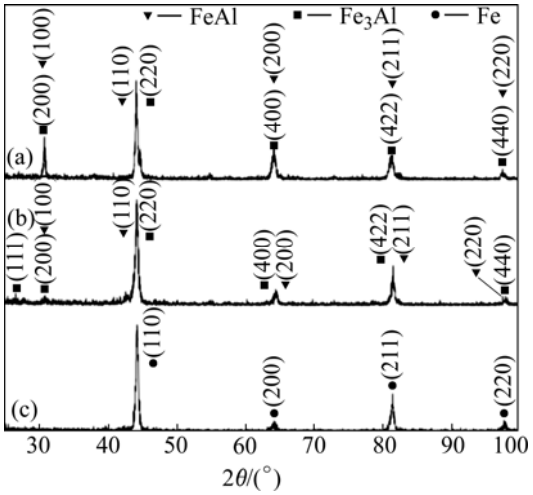

Fig.3 X-ray patterns of aluminized layer: (a) Surface; (b) 55 μm from surface; (c) 175 μm from surface

Fe_3Al. The DO_3 structure is transferred from $B2$ structure due to ordering of the compound and all the peaks from $B2$ structure in XRD patterns overlap with the peaks from DO_3. Only a few characteristic peaks from DO_3 structure (such as (111) peak) does not overlap with the peaks from $B2$. In Fig.3(a), it seems difficult to determine weather the intermetallic compound in the sedimentary layer has DO_3 or $B2$ structure. However, the result of microanalysis shows that the aluminum content in the sedimentary layer varies from 60% to 35% (in molar percentage) and the compound should be in the FeAl single phase area according to the Fe-Al binary phase diagram. Thus it is believed that the sedimentary layer mainly consists of FeAl compound with $B2$ structure.

Under the sedimentary layer is the diffusion layer and the reduction of Al content becomes gradual as shown in Fig.2(b). The XRD pattern taken from the sample, of which a layer of 55 μm thick from the surface of the aluminized sample was removed by grinding, is shown in Fig.3(b). It can be seen that there is a characteristic peak indexed as arising from (111) plane of Fe_3Al with DO_3 structure, although the intensity of the peak is very low. The other peaks are similar with those in Fig.3(a). The aluminum content in the diffusion layer, determined by EDS, is approximately 26%, close to that of Fe_3Al. Therefore, the Fe-Al compound in the diffusion layer can be identified as Fe_3Al. As the ordering transformation of Fe_3Al from $B2$ structure to DO_3 structure takes a long period (100 h, at 550 ℃[9]), the Fe_3Al compound in diffusion layer might have a structure which is not completely ordered (from $B2$ to DO_3). Fig.3(c) shows XRD pattern taken from the sample, of which a 175 μm-thick layer is removed from the aluminized surface. In this pattern the peaks arising from Fe-Al intermetallic compound have disappeared and the remaining peaks are indexed as arising from the α-Fe phase. From the image shown in Fig.1, it can be measured that the total thickness of the surface film, including sedimentary and diffusion layers, is about 180 μm. As a 175 μm-thick layer is removed from the surface of this sample, the polished surface of the sample analyzed is located in the bottom of the diffusion layer in the original sample. The result of microanalysis shows that the aluminum content in this layer is about 5.44%, within the range of aluminum solubility in α-Fe phase. This is consistent with the XRD pattern shown in Fig.3(c).

3.3 Discussion

In the present work, the aluminizing treatment is carried out at 950 ℃, much higher than the melting point of pure aluminum. During the treatment, hence, the sedimentary Al covers all the surface of 45 steel substrate. The solubility of Fe is up to 44% in the liquid aluminum, much higher than the solubility of Fe in solid aluminum (about 0.02%[10]). Therefore, iron atoms soon dissolve into the liquid aluminum layer and react with aluminum to form Fe-Al compounds. Since all the Fe-Al intermetallic compounds have higher melting point than that of aluminum, the formation of Fe-Al compounds causes the solidification of liquid phase on the sample surface. The sample is still at very high temperature after the liquid phase solidifies and aluminum atoms diffuse from surface layer to substrate along the defects and grain boundary. Meanwhile, iron atoms diffuse along opposite direction, resulting in the reaction between aluminum and iron as well as the formation of Fe-Al compounds underneath the surface. This is the course of diffusion—reaction[10−11]. The gradient of aluminum content and diffusion—reaction lead to the formation of three layers on the sample surface as shown in Fig.1. According to Fe-Al binary diagram, five types of intermetallic compounds (Fe_3Al, FeAl, $FeAl_2$, Fe_2Al_5 and $FeAl_3$) might appear in the Fe-Al binary alloys. The previous studies[12−13] reported that the aluminum-rich compounds (Fe_2Al_5 and $FeAl_3$) were observed in the carbon steel samples using the technique of thermal infusion calorization. However, the aluminum-rich Fe-Al compounds do not appear in the samples prepared by double glow plasma aluminizing in the present work, indicating that different microstructures and intermetallic compounds will form when different techniques are used. Particles with very high energy bombard the surface of samples during aluminizing treatment, generating large amount of dislocations and vacancies[14] in the surface layer of the sample, which accelerates the diffusion of aluminum. Moreover, the aluminum deposition process during double glow plasma aluminizing is slower than that in thermal infusion calorization. The two factors, fast diffusion of aluminum towards to the inner of the

substrate and gradual deposition of aluminum on the sample surface, lead to the formation of Fe-rich intermetallic compounds, rather than Al-rich intermediate phases.

3.4 Nano-indentation analysis

The traditional method of hardness testing is pressing an indenter with specific shape and size into the sample, and then measuring the size of the indentation that the indenter has left when the loading on the press is removed. The size of the indentation measured is the attribute of the hardness. If the surface of the sample has layered structure, it is not reasonable to test the hardness of sample surface by traditional method. Nano-indentation analysis is a technique, in which the numerical value of loading and displacement of the indenter are continuously recorded. The hardness is treated as the function of indentation depth. Both plastic and elastic deformation are recorded during testing and micro-hardness and elastic modulus can be obtained when this method is used.

In the present work, the surface hardness of aluminized samples was measured using the nano-indentation analysis and the results are shown in Fig.4. For 45 steel substrate, the dynamic hardness obtained is 1.22 GPa at the depth of 0.59 μm. Hereafter, the micro-hardness keeps stable when indenter depth increases. The dynamic hardness of the aluminized layer is significantly higher than that of the substrate when the indenter just contacts the surface of the sample. This might be accounted for the effect of surface state. With the increase of indention depth, the micro-hardness of the sample decreases rapidly. When the indention depth is 0.85 μm, the reduction of micro-harness becomes slowly, indicating that the effect of the surface sensitivity on the micro-hardness of aluminized layer is weakened. Even though, the micro-hardness is much higher than that of the steel substrate when the hardness of both samples reaches the stable state. In addition, the indentation depth

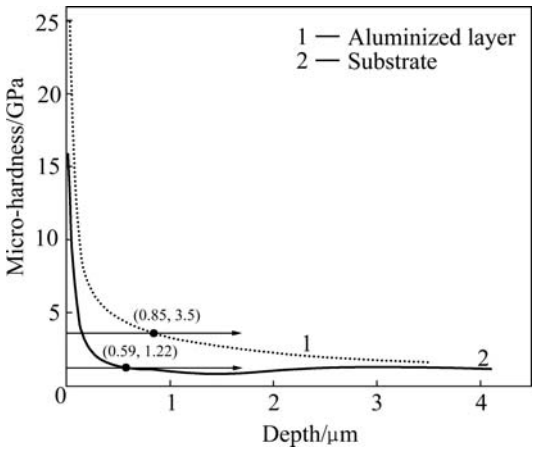

Fig.4 Dynamic hardness of different samples

of the aluminized layer is much smaller in comparison with that of the substrate, indicating that the formation of Fe-Al compounds is effective in increasing the surface hardness of steel samples. The average elastic moduli of the aluminized layer and substrate are 176 GPa and 94.3 GPa, respectively, determined by the load—unload curves. The large difference on elastic modulus between aluminized layer and steel substrate implies that the sample has high anti-deformation ability after aluminizing treatment.

3.5 Corrosion behavior of aluminized layer

S^{2-} and Cl^{-} ions are the common corrosive ions in petrochemical and chemical industry. The previous studies show that Fe-Al intermetallics have good corrosion resistance in the environment of vulcanized gases and molten salt of sulfate or chloride. However, the corrosion behavior of Fe-Al compounds in aqueous solution containing S^{2-} or Cl^{-} ions has not been systematically reported. In the present work, the electro-chemical corrosion tests were conducted on the surface aluminized samples in comparison with 1Cr18Ni9Ti stainless steel as well as 45 steel. Figs.5(a) and 5(b) show the polarization curves obtained from samples prepared in the present work and comparative steel samples in two corrosive solutions. The kinetic parameters (corrosion potential φ_{corr}, corrosion current density J_{corr}, and passivation current density J_{pass}, the minimum current density in passivation region) are derived from the polarization curves and summarized in Tables 2 and 3.

From the anodic polarization curves (Fig.5(a)), it can be clearly seen that the aluminized layer behaves actively and the current density increases gradually with the rise of potential. As soon as the anodic potential reach −0.880 V, the current density decreases sharply, indicating that a passivating film forms on the sample surface. Whereafter, the current density increases again when the potential is as high as −0.491 V. The re-increase of current density implies that the passivating film is broken down and a new circle of anodic dissolution takes place. The secondary passivation occurs when the potential reaches −0.361 V. Here, the corrosion current density is rather small (1.004 mA/cm^2) and does not show apparent increase with the increase of potential. This indicates that the system goes into a stable state of passivation. From Table 2, it can be seen that the aluminized sample shows better corrosion resistance than 45 steel. The corrosion rate of the aluminized sample is about 1/6 that of 45 steel. In comparison with stainless steel, however, the aluminized layer has a broader passivation region and a much smaller corrosion current density when the potential is over 0.042 V.

Chloride solution has the maximal corrosion to

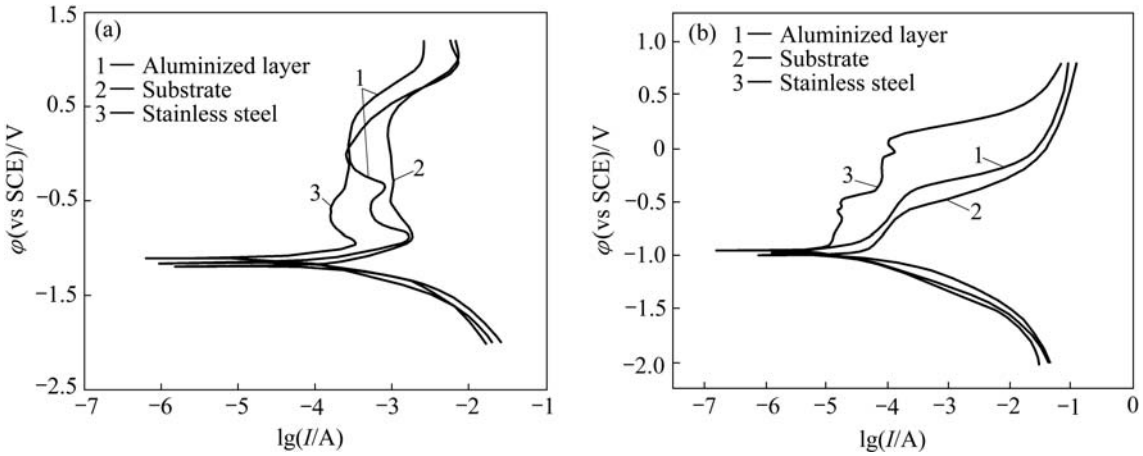

Fig.5 Comparative polarization curves for different samples in 2.0%Na_2S solution (a) and 0.05 mol/L Na_2SO_4 + 0.5 mol/L NaCl mixed solution (b)

Table 2 Electrochemical parameters of different samples in 2.0% Na_2S solution

Specimen	φ_{corr}/V	J_{corr}/(mA·cm^{-2})	J_{pass}/(mA·cm^{-2})	Corrosion rate/(g·m^{-2}·h^{-1})	Relative corrosion rate
Aluminized layer	−1.151	1.416	1.004	4.755	1.00
45 steel	−1.192	2.859	3.633	29.870	6.28
Stainless steel	−1.100	0.227	0.519	2.372	0.50

Table 3 Electrochemical parameters of different samples in mixed solution of 0.05 mol/L Na_2SO_4 and 0.5 mol/L NaCl

Specimen	φ_{corr}/V	J_{corr}/(mA·cm^{-2})	Corrosion rate/(g·m^{-2}·h^{-1})	Relative corrosion rate
Aluminized layer	−0.958	0.114	0.383	1.00
45 steel	−1.003	0.559	5.840	15.25
Stainless steel	−0.958	0.069	0.721	1.88

metal because of the special destructive action that halide ions can easily penetrate the passive film[15] due to their small radius. The polarization curves (Fig.5(b)) of three samples in 0.05 mol/L Na_2SO_4 and 0.5 mol/L NaCl mixed solution show that the aluminized layer and 45 steel behave actively in the solution and it seems there is no passivation occurring. The stainless steel, however, exhibits an unstable passivation state at potential of −0.889 V due to the addition of Cr in the steel, which protects the passivation film from the Cl^- containing aggressive environment. Table 3 shows that the corrosion potentials of aluminized sample and stainless steel are at the same level, indicating that the two samples have the same tendency when being corroded in this solution. Although the corrosion current density of aluminized layer is larger than that of stainless steel, the corrosion rate of the former is smaller than that of the later because of the different corrosion ions. In comparison with 45 steel, the anodic polarization curve of aluminized layer lies on the left upper side, reflecting that the aluminized layer has a smaller corrosion current density than substrate at the same potential, but higher potential at the same current density. This implies the better corrosion resistance of alloyed layer than 45 steel in the Cl^- containing solution. The corrosion potential of 45 steel is 45 mV lower, while the corrosion current density is 5 times that of aluminized layer. The corrosion rate of 45 steel is 15 times that of aluminized sample, which exhibits that the technique of double glow plasma aluminizing is very effective in improving the corrosion resistance.

4 Conclusions

1) A protective film on the surface of 45 steel has been synthesized by using the technique of double glow plasma surface aluminizing. The surface film prepared is composed of a sedimentary layer and a diffusion layer, with a total thickness of about 180 μm. The microstructure of both layers consists of the Fe-Al intermetallic compound, which is FeAl with *B*2 structure in the sedimentary layer and Fe_3Al with incompletely ordered DO_3 structure in the diffusion layer. The protective film exhibits high micro-hardness and very good metallurgical bonding with the substrate.

2) In comparison with the substrate of 45 steel, the

aluminized sample shows much higher corrosion resistance in 2.0% Na_2S and 0.05 mol/L Na_2SO_4 + 0.5 mol/L NaCl mixed solutions.

References

[1] LIU Feng-xiao, HUANG Bai-yun, ZHOU Ke-chao, LIU Yong, CHEN Jian-xun. Present status and future prospects of FeAl alloy [J]. Materials Science and Engineering of Powder Metallurgy, 2000, 5(3): 193−200. (in Chinese)

[2] SUN Yang-shan, YU Xin-quan, XUE Feng, MEI Jian-ping, HUANG Hai-bo, WANG Shi-qin. Study of Fe_3Al-based intermetallics [J]. Materials Review, 2000, 11(8): 66−67. (in Chinese)

[3] DEEVI S D, HAJALIGOL M R, CLIFF LILLY A, FLEISCHHAUER G S. Development and production of FeAl-based intermetallic alloys [J]. Trans Nonferrous Met Soc China, 1999, 9(1): 309−317.

[4] LINS V F C, FREITAS M A, SILVA E M P. Corrosion resistance study of Fe-Mn-Al-C alloys using immersion and potentiostatic tests [J]. Applied Surface Science, 2005, 250(1/4): 124−134.

[5] SRIRAM S, BALASUBRAMANIAM R, MUNGOLE M N, BHARAGAVA S, BALIGIDAD R G. Effect of cerium addition on the corrosion behaviour of carbon-alloyed iron aluminides [J]. Corrosion Science, 2006, 48(5): 1059−1074.

[6] LUU W C, CHIANG W C, WU J K. Effect of Cr and Ti additions on the corrosion behavior of Fe_3Al alloys in chloride-containing sulfuric acid solutions [J]. Materials Letters, 2005, 59(26): 3295−3298.

[7] REGINA J R, DUPONT J N, MARDER A R. Gaseous corrosion resistance of Fe-Al based alloys containing Cr additions (Part Ⅰ): Kinetic results [J]. Materials Science and Engineering A, 2005, 404(1/2): 71−78.

[8] ZHANG Wei, WEN Jiu-ba, WANG Xiao-feng, XIONG Fei, CUI Xin-an. $AlFe_3C_{0.5}$ phase in diffusion layers of hot dip aluminized steel [J]. The Chinese Journal of Nonferrous Metals, 2007, 17(10): 1632−1636. (in Chinese)

[9] MA Hong-tao. Prepation and study of friction and wear mechanism of Fe-Al intermetallic base friction material [D]. Shandong: Shandong University, 2005: 45−48. (in Chinese)

[10] WANG Xing-qing, SUI Yong-jiang, LU Hai-bo. Fe and Al atoms diffusion in intermetallic formation [J]. Journal of Shanghai University (Natural Science), 1998, 4(6): 661−667. (in Chinese)

[11] SKOGLUND H, KNUTSON-WEDEL M, KARLSSON B. Diffusion of Al during hot consolidation of FeAl [J]. Acta Materialia, 2006, 54(15): 3853−3861.

[12] KOBAYASHI S, YAKOU T. Control of intermetallic compound layers at interface between steel and aluminum by diffusion-treatment [J]. Materials Science and Engineering A, 2002, 338(1/2): 44−53.

[13] XIA Yuan, YAO Mei, LI Tie-fan. Coating formation process and microstructure during hot dip aluminizing (HDA) on steel [J]. The Chinese Journal of Nonferrous Metals, 1997, 7(4): 154−158. (in Chinese)

[14] ZHANG Ping-ze. Double glow plasma surface alloying burn-resistant titanium alloy [D]. Taiyuan: Taiyuan University of Technology, 2004: 79−106. (in Chinese)

[15] WANG Zhen-xia. Study on processing and surface properties of plasma surface niobium alloying on Ti6Al4V and pure titanium. [D]. Taiyuan: Taiyuan University of Technology, 2006: 59−61. (in Chinese)

(Edited by YANG Bing)